NEW IMPROVED SYSTEM FOR WWVB BROADCAST

John Lowe, Matt Deutch, Glenn Nelson, Douglas Sutton, William Yates
National Institute of Standards and Technology
E-mail: *John.Lowe@NIST.gov*

Peder Hansen
SPAWAR Systems Center Pacific, U. S. Navy
E-mail: *Peder.Hansen@Navy.mil*

Oren Eliezer[1], Tom Jung[1], Stephen Morrison[1], Yingsi Liang[1,2], Dinesh Rajan[2], Sidharth Balasubramanian[1,3], Arun Ramasami[1,3], Waleed Khalil[3]
[1]Xtendwave, [2]Southern Methodist University, [3]The Ohio State University
E-mail: *OEliezer@Xtendwave.com*

Abstract

The WWVB broadcast of the time-code signal has undergone no major changes in its communications protocol and modulation scheme since its introduction in 1963. Its amplitude-modulation (AM) and pulse-width based representations of its digital symbols were designed to allow for a simple low-cost realization of a receiver based on envelope detection, widely used with AM audio broadcasting at the time, whereas present day technology allows much more efficient methods for modulation/demodulation to be realized at low cost. Over a decade ago, the station's power was significantly increased, allowing the broadcast from Colorado to effectively cover most of North America. This has spurred the popularity of radio-controlled clocks and watches, more commonly known as "atomic clocks." However, electromagnetic interference (EMI) experienced in typical residential and office environments can make it difficult to receive the WWVB signal in various locations, and particularly on the East Coast, where on-frequency interference from the MSF station in the UK is received at relatively high levels.

The new protocol and modulation scheme being introduced by NIST effectively addresses these problems, and will enable greatly improved reception of the WWVB broadcast without affecting existing devices. This backward-compatibility is achieved by maintaining the existing AM characteristics while adding various new features through phase modulation (PM).

While the new protocol can provide improved timing resolution, it was designed primarily to enhance the system's robustness by reducing the signal-to-interference-and-noise-ratio (SINR) required for reception, to provide much improved coverage and to enable new applications. Although the demodulation of the signal's phase involves greater complexity, today's technology allows for such implementation to be realized in a low-cost integrated circuit.

Analyses are presented, including simulated and measured results, to illustrate the challenges encountered in existing receivers. The new modulation scheme and protocol are described and are shown to be effective in addressing these challenges, resulting in several orders of magnitude in performance improvements.

INTRODUCTION

The National Institute of Standards and Technology (NIST) operates radio station WWVB, a low frequency (LF) broadcast of standard time and frequency. The station, located north of Ft. Collins, Colorado, started broadcasting a 60 kHz signal at 5 kW of power in 1963, serving as a frequency standard.

Pulse-width amplitude modulation (AM) was added 2 years later by use of a binary coded decimal (BCD) format, allowing the reception of a time-of-day code. However, it was not widely used, due to the low field strength. A major upgrade was completed in 1999 that increased the effective radiated power to 50 kW **[1]** and subsequently to 70 kW in 2006. The high-power digital broadcast created a commercial market for time-of-day radio-controlled clock (RCC) devices such as wall clocks, alarm clocks and wristwatches that now number in the millions **[2]**. However, these devices have been subject to technical limitations that have prevented the WWVB broadcast from penetrating the commercial market beyond the novelty of self-setting clocks and watches. NIST has been investigating various approaches to effectively address such problems so as to allow for wider use of the WWVB broadcast in various applications **[3]**.

FACTORS HINDERING RECEPTION

Various factors exist that may hinder reception in different ways. These may be divided into passive factors (i.e., losses) and active factors (i.e., interference sources). This section lists these factors, as the understanding of their characteristics is essential when developing a solution to address them.

PROPAGATION LOSSES

One well-known limitation arises from the nature of the LF signal's propagation. The sun's effect on the ionosphere causes a diurnal variation in signal strength that limits daytime reception. This is why most commercial RCC devices can receive only at night. Figure 1 compares the calculated day and night coverage areas of WWVB, when assuming a field intensity of 100 μV/m, which is barely sufficient for reception in most consumer-market devices.

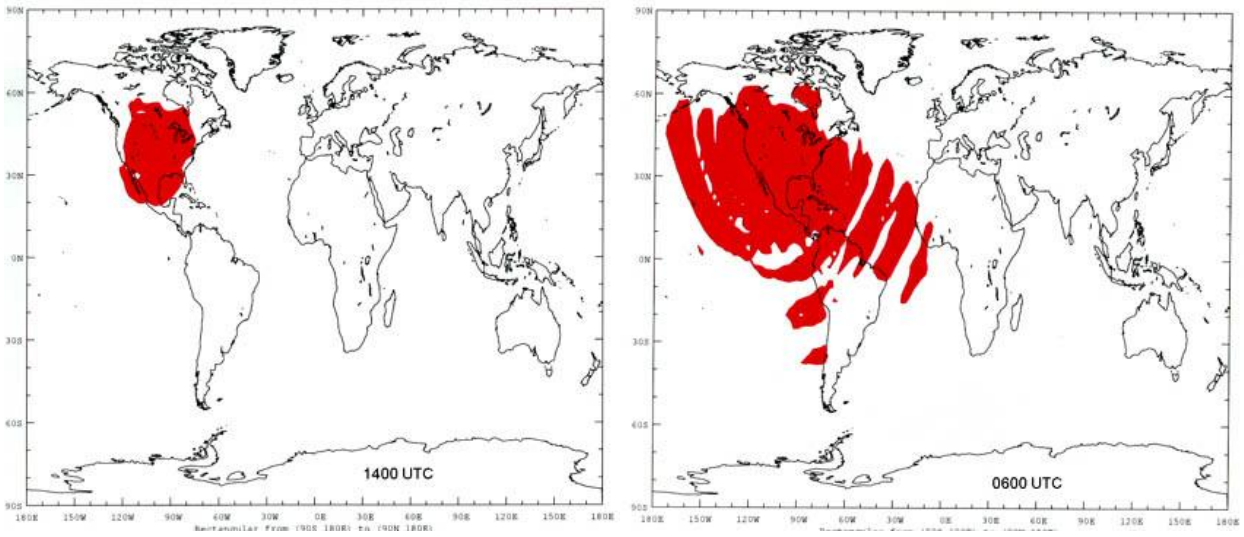

Daylight Coverage Area Nighttime Coverage Area

Figure 1. WWVB coverage at a 100 μV/m level.

Such field intensity, when coupled with the gain of typical ferrite-rod based antennas that are used in common commercial RCC devices, results in an input signal level that is below 1 μV, which is on the order of the sensitivity level specified by vendors of receivers. While this signal level may be sufficient when assuming that the only noise at the receiver is the natural thermal noise, whose bandwidth is typically limited within the receivers by a crystal with a bandwidth on the order of 10 Hz, the presence of additional interference may require a much higher signal level for proper reception.

The WWVB signal must serve at least the Continental United States (CONUS). There is some variability in signal strength with range but, in general, the signal is weaker at longer ranges. Thus, the most challenging locations in CONUS are southern Florida (~ 2700 km) and northern Maine (~ 3,000 km). As seen in Figure 1, the signal in these areas during the day may be very weak due to absorption in the ionosphere. At night, however, the ionization decreases, reducing absorption and resulting in better long range propagation **[4]**.

OBSTRUCTION, MULTIPATH AND SHADOWING/SHIELDING

Multipath propagation, which is experienced when a receiving device receives the signal from different paths, such as when reflected off nearby objects, is a well-known phenomenon in wireless communications. At 60 kHz propagation is best described as using the Earth and ionosphere as a waveguide. This type of propagation experiences a similar phenomenon in that several modes are present and sometimes add destructively, resulting in a temporary reception null at a given range from the transmitter. Figure 2 shows the typical signal strength for an all-night path from WWVB in the direction of Washington, DC. The plot units are dB μV/m, with 40 dB μV/m corresponding to 100 μV/m. The range to Washington is approximately 2400 km, where a modal interference null is shown to occur, bringing the signal down below 100 μV/m. These nulls vary in position and depth as the ionosphere varies over time so that the signal is not always weak in that area. In general, the signal level varies more in the vicinity of a null, so the ability to receive in those locations will vary more over time.

In addition to the losses associated with the distance and the topography, a receiving device may be challenged by further attenuation that is caused by shielding effects, such as structures and objects that create "shadows" in the electromagnetic field. Structures rich with metallic elements, such as office buildings, which may be in the propagation path can represent obstructions, and the placement of a receiving device in a closed environment (office, warehouse, etc.), where it may be surrounded by such obstructions, subjects it to a form of shielding. A measurement performed at Xtendwave's offices, located on the 10th floor of a building in Dallas, revealed as much as 20 dB difference between the signal level received on the window-ledge facing north versus the level measured about 5 meters inside the office space, while holding the antenna at the same optimal orientation. This result is shown in Figure 3, where the two spectra are captured by use of the same parameters and within a minute apart. It is to be noted that the window frames were metallic, as well as the beams holding the internal sheetrock walls and the exterior of the building, contrary to the wooden infrastructure typically used in American residential houses, where a lesser shielding effect is to be expected.

ORIENTATION OF THE RECEIVING ANTENNA

The antennas used in consumer-market devices are very small with respect to the wavelength but they are not isotropic or omni-directional. Typically being based on a ferrite rod, they are essentially a magnetic dipole for which the antenna pattern exhibits nulls in the two directions pointed by the rod. For optimum reception the ferrite rod should be oriented broadside towards Fort Collins. In practice, when users hang a clock on a wall in their house, they might not be able or interested in relocating it to where its orientation approaches the optimal one. Consequently, a random orientation angle θ must be assumed for this link, potentially introducing a significant loss in the amplitude of the received signal, corresponding to the factor

$\cos\theta$. If a uniform distribution is to be assumed for θ, then amongst a large population of users, it can be shown that about 30% would be experiencing at least 6 dB of power loss with respect to the optimal orientation, about 20% would be losing over 10 dB, and over 10% would be losing over 15 dB of signal power. This means that in order to ensure coverage at a certain location with a probability above 90%, the field intensity around the receiver must consider an additional margin of 15 dB on top of whatever other margin may be allocated to the other factors that hinder reception.

ATMOSPHERIC NOISE

Lightning represents a strong noise source in the LF band, and is worse at the lower frequencies, where even distant lightning storms worldwide contribute to the atmospheric noise floor induced in the receiving antenna. At 60 kHz the atmospheric noise levels are typically 100 dB greater than thermal noise, when assuming a theoretical antenna of 0 dBi gain **[5]**. However, the electrically and physically small receiving antennas, of the type typically found in RCC commercial products, are very lossy, and the level of atmospheric noise received in them is attenuated to the point that it is below the thermal noise in the receiver's front-end. Lightening originating from nearby locations may still represent a dominant interferer of impulsive nature, for which a portion of a received frame may be corrupted. In existing products, the frame part remaining intact may be useless in extracting the correct time, resulting in complete reception failure. Error-correcting codes, based on adding redundant bits in the transmitted message, allow for the recovery of erroneous bits in the receiver, and, hence, are an effective way to address such interference, but they were not employed in the historical WWVB broadcast.

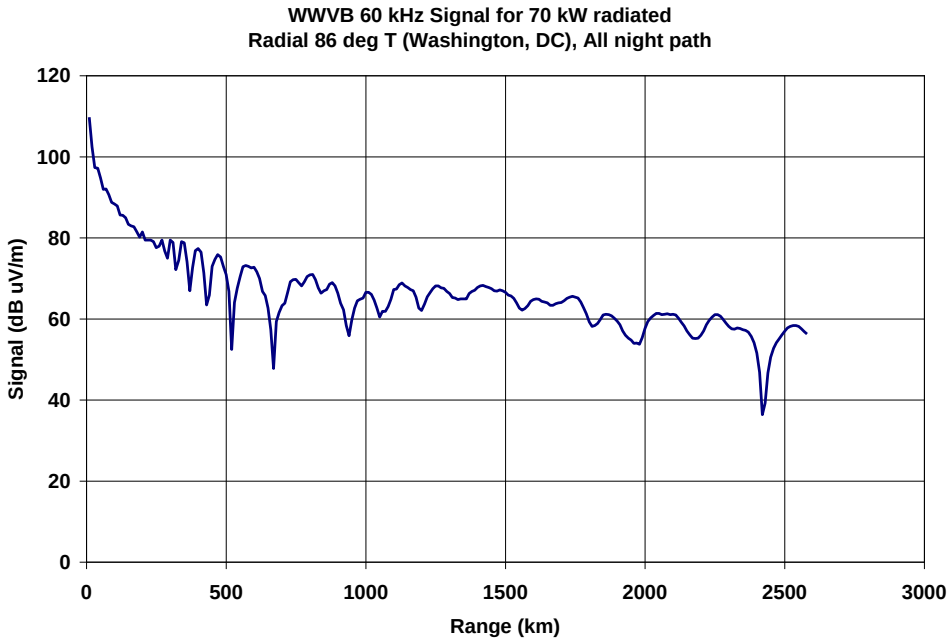

Figure 2. Signal strength from WWVB in direction of Washington, D.C.

MAN-MADE NOISE

Man-made noise (MMN), which is typically created by electrical appliances and electronic devices operated by humans, is an increasing source of electromagnetic interference (EMI), as the number of personal computers, handheld devices, and various consumer-market electronics found in industrial, office and residential environments, continues to grow. The circuitry in these devices, containing switched-mode power supplies, digital circuitry operating at certain clock frequencies, etc., can create energy around 60 kHz, which may be emitted and received by a victim RCC at a level that is considerably higher than that

of the natural noise floor. In particular, the harmonics of power equipment operating at 60 Hz, as well as the raster scan rate of some video monitors, are common sources of EMI at 60 kHz. Although regulations exist for the maximum allowed level of non-intentional emissions for devices that undergo an approval procedure, these focus on higher frequencies, where more conventional communication systems may be impacted. Furthermore, the appliances and machinery, including elevators that create noise due to their use of electric motors, may emit high levels of noise at low frequencies, without this originating from electronic circuitry.

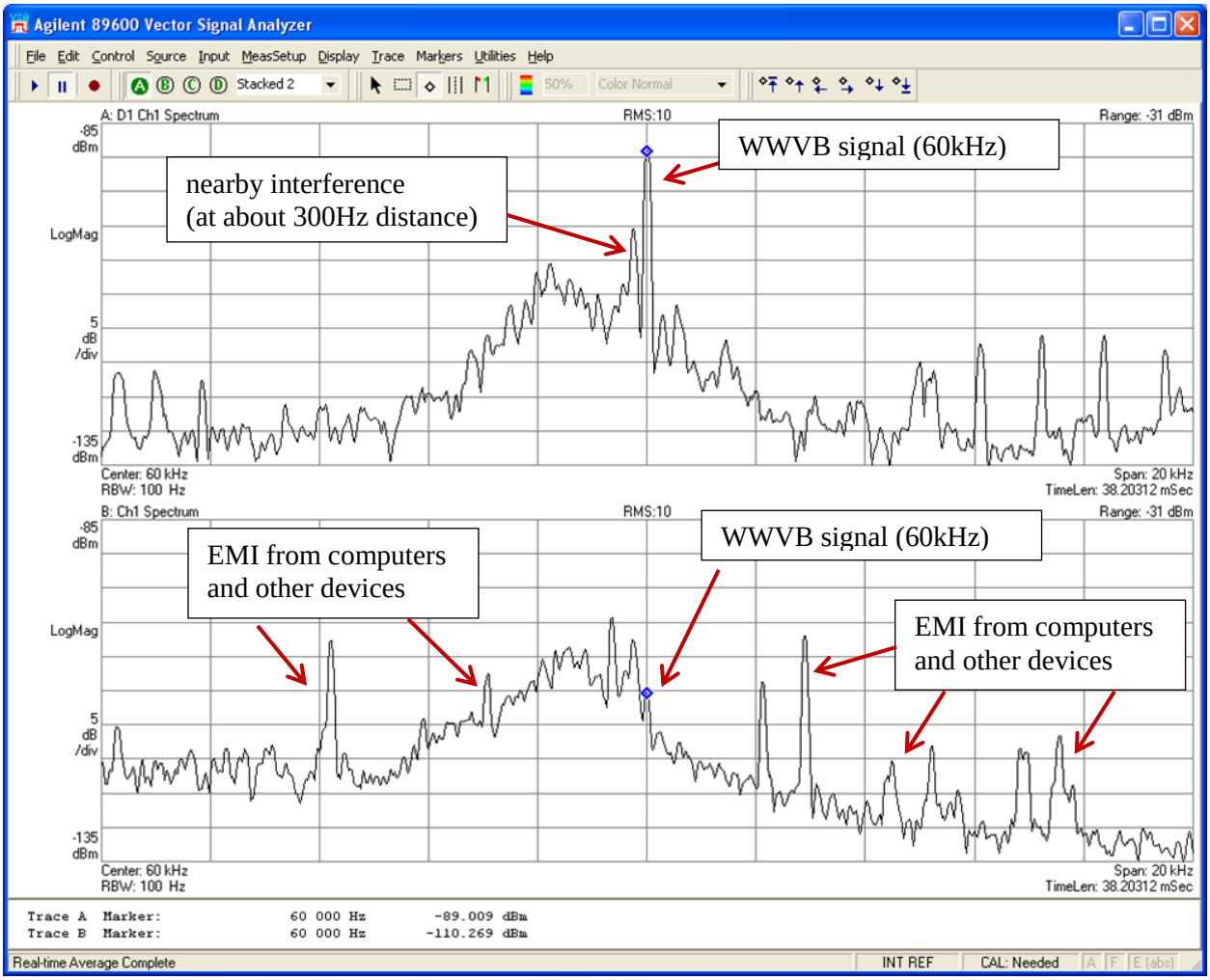

Figure 3. Measured EMI around 60 kHz and the WWVB signal in an office environment in Dallas (top: at the office window facing Colorado, bottom: a few meters into the office/lab area). Sweep: 50 to 70 kHz (2 kHz/division), Amplitude: 10 dB/division (bottom= -135 dBm), RBW: 100 Hz.

In practice, inhabited environments typically contain sources of locally high levels of MMN that can pose a significant challenge for RCC devices. It is for this reason that user manuals of many RCC products recommend placing them far from potential sources of interference, which is not always practical, since users may be unable to avoid interference in a location of interest or simply disregard the instructions. Figure 3 shows the levels of MMN captured around noontime in a large ferrite rod antenna matched to an impedance of 50 Ω. It was placed in an office environment in Dallas both inside the office, closer to multiple electronic devices (bottom plot), as well as closer to the window, further away from the sources of

interference (top plot). The spectra captured in Figure 3were measured by use of a frequency span of 20 kHz around 60 kHz and a resolution bandwidth (RBW) of 100 Hz, for which the theoretical thermal noise floor is -154 dBm/Hz. As can be seen in the bottom figure, the level of MMN inside the office, close to the PC and other devices, was above -130 dBm/Hz, more than 2 orders of magnitude worse than what may be experienced in a perfectly quiet environment. The WWVB signal is shown to be much lower there, apparently due to shielding effects, whereas the measurement shown in the top plot, taken by the window, reveals a received signal around -90 dBm. This experiment demonstrates how different the conditions may be for RCC devices that are placed in the same office or home space, while maintaining the same antenna orientation.

It is to be noted that the antenna used in this experiment was larger than what is typically found in a consumer-market product, but while this affects the absolute signal levels shown in Figure 3, it does not affect the relationship between the two. Repeated experiments performed with several commercially available wall-clocks have shown strong correlation with these findings: i.e., a high rate of successful receptions by the window versus repeated failures deeper in the office. This indicates that the measured difference between the tested locations is sufficient to result, in practice, in a noticeable impact on user-perceived performance.

RADIO FREQUENCY INTERFERENCE (RFI)

The term radio-frequency interference (RFI) is typically used in scenarios whenever the source of interference is a known or intentional emitter operating at a frequency that may interfere with the receiving device of interest. This is unlike EMI, where the emissions causing interference are unintended or unknown. It is believed that a source of RFI, at least on the eastern seaboard of the CONUS, is the frequency-coherent sister station MSF (historically called "Rugby," although it is now located in Anthorn) operated by the National Physical Laboratory (NPL) in the United Kingdom. Both stations broadcast a pulse-width AM signal at a 1 Hz rate on a 60 kHz carrier **[6,7]**. The detection of the WWVB signal, typically performed by an envelope detector, is significantly limited in the presence of such an interfering signal.

Figure 4 shows the estimated signal-to-jammer (*S/J*) ratio in terms of the field intensity relationship, with *S* corresponding to WWVB and *J* to MSF, for three locations on the East Coast over the course of a day. Negative values correspond to instances when the MSF jammer creates a stronger electromagnetic field than that of WWVB. When considering the directionality of the receiving antenna, the *S/J* relationship between the electrical signals in the receiver can deviate from these values according to the arbitrary orientation at which the user may be placing an RCC device.

If the RCC orientation is such that it is directed towards the UK, while the null in its radiation pattern is directed towards Fort Collins, the effective *S/J* ratio will not be that of the field intensities, but may be orders of magnitude worse. Consequently, even for those instances for which Figure 4 estimates *S/J* = 20 dB, it is likely that some percentage of devices actually experience a much lower ratio, potentially below the threshold required for their proper operation.

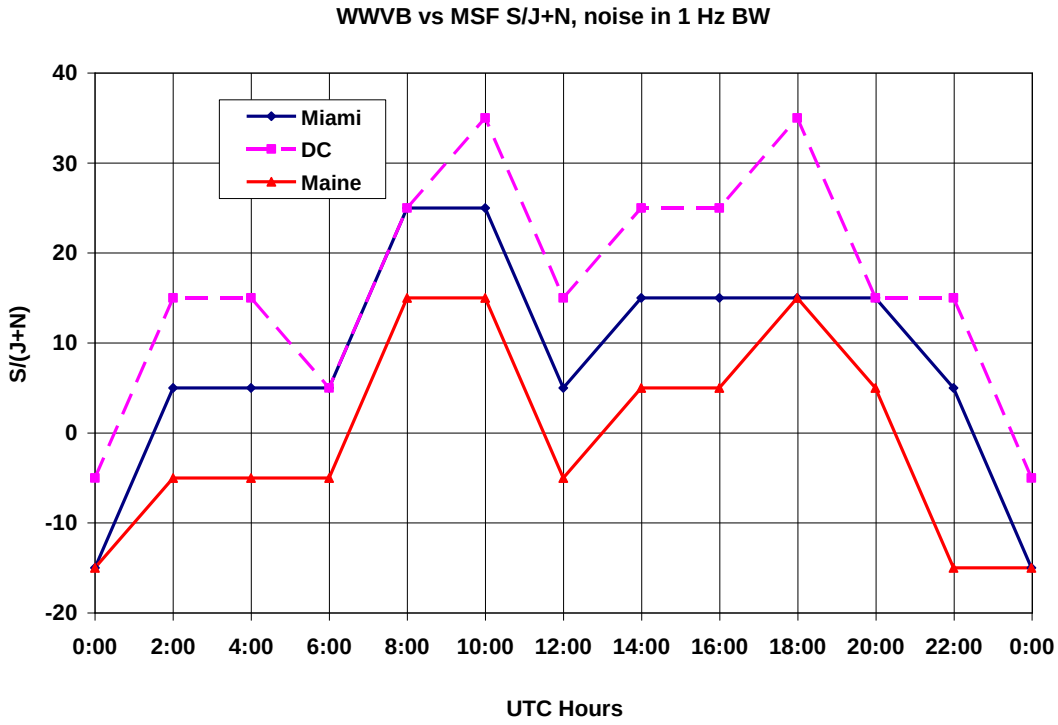

Figure 4. Estimated on-frequency interference from MSF during the course of one day.

Figure 5 provides a simplified block diagram for an envelope-detector-based receiver of the type that is typically used in the consumer market RCC devices. As can be seen in this block diagram, the AM signal is converted into an analog equivalent baseband signal by use of a conventional nonlinear envelope detector (similar to the diode-based circuit in traditional AM receivers). A threshold operation that follows serves to determine the middle level, around which the voltages below it would be converted to a logical low level and the voltages above it to a logical high level. The digital processing stage that follows this operation measures the pulse durations and decides on the recovered symbols ('1', '0', or 'marker'). Naturally, with such receiver topology, an on-frequency interferer that is present while the WWVB victim signal in the receiver is at its "low" state can cause the receiver to decode that symbol incorrectly. In particular, the 'marker' symbols in WWVB are represented by 0.8 s of a low-level in the carrier (-17 dB) followed by 0.2 s at the high level, and are used to indicate the timing of the minute frame and the fields within it **[8]**.

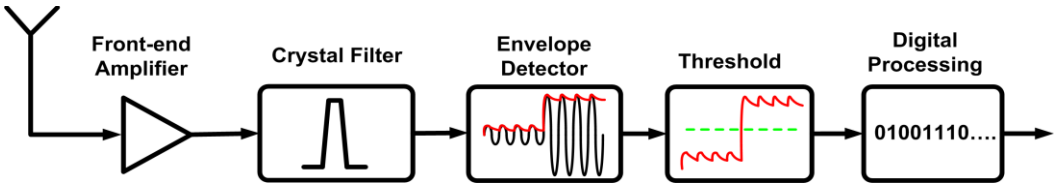

Figure 5. Existing receiver architecture.

Figure 6 illustrates the principle of operation of a typical envelope-detection-based receiver. The modulated signal on the left, which is the input to the receiver, is shown in the absence of additive noise, and has two different amplitude levels, with the information represented in the durations of each of these levels. The modulation rate and carrier are not to scale, for the sake of visual clarity, which is why the decay time of the envelope detector in the middle figure appears too long with the respect to the pulse duration. The figure on

the right illustrates how the high/low decision is made, by following the "low" and "high" levels with dedicated peak holders (with appropriate time-constants) and deriving the middle (average) of these two. A threshold operation (i.e., simple comparator) is then used to create the logic level signals for the digital stage that follows, where the pulse durations are measured and the '1'/'0'/'marker' symbol decision is made.

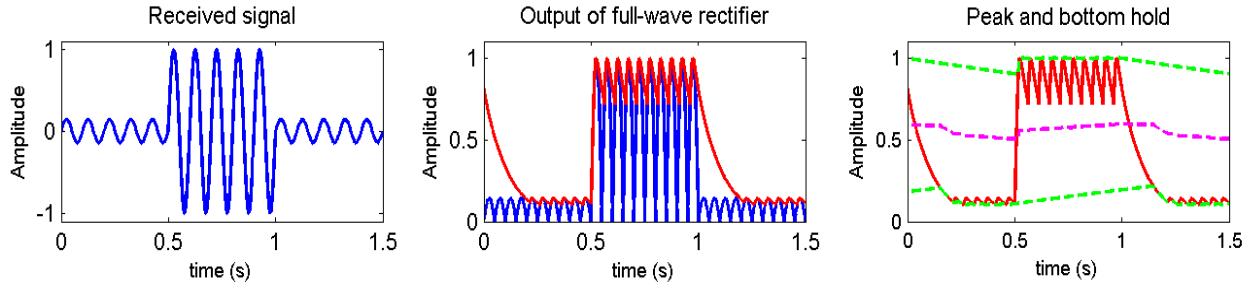

Figure 6. The analog processing of the AM signal in a typical WWVB receiver.

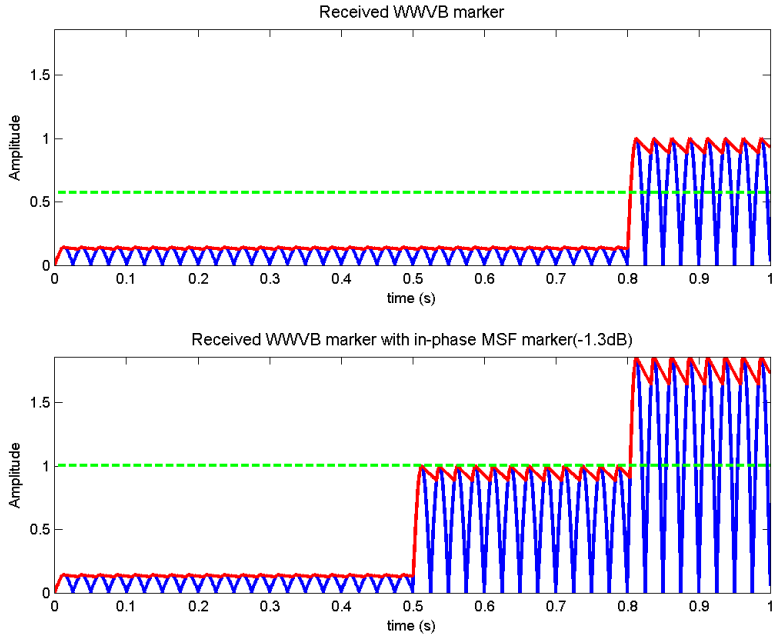

Figure 7. The effect of an in-phase MSF interferer with 86 % relative amplitude (-1.3 dB).

Figure 7 illustrates how the threshold operation can be misled by the presence of a jammer having the nature of the MSF signal. With the high and low amplitude levels in the WWVB signal having a ratio of 1/7 (-17 dB), the lower level is shown to be at 0.14 (with the high level normalized to 1), and the threshold is set to the middle value of (1 + 0.14) / 2 = 0.57. The WWVB signal shown in the top figure is a marker, having a low level of 0.8 s followed by a high level of 0.2 s. The additive in-phase MSF signal shown in the bottom figure, for the first marker in a minute, has a low level of 0 for the first 0.5s of the second and a high level assumed to be 86 % (-1.3 dB) relative to the WWVB signal. The three different sum results shown for $0 < t < 0.2$ s, 0.2 s $< t < 0.5$ s, and 0.5 s $< t < 0.8$ s are shown to be 0.14, 1, and 1.86 respectively. The maximum and minimum peak holders for these three levels would produce a middle level that is around (1.86 + 0.14) / 2 = 1, for which the signal may be high for $t > 0.5$ s. Consequently, even in the absence of noise, the threshold decision operation will fail for that interval and the digital stage that follows would be

decoding this symbol as a '1' instead of 'marker'.

To conclude, even in the absence of additive noise (i.e., very high SNR), with an in-phase interfering MSF signal that is **1.3 dB** below the WWVB received signal or stronger, an envelope-detector-based receiver would fail to correctly decode the received WWVB signal. For the other extreme case of out-of-phase interference (180° phase difference), the effect of the interferer is worse, resulting in a maximal tolerable interfering level that is about **6.5 dB** below the received WWVB signal level. Between these two phase relationships, the tolerable level of the MSF interferer is between these two values. It is to be noted that when the SNR is not very high, a receiver's performance may be noticeably degraded by the presence of this jammer, as it effectively reduces the noise margin in its decision function. The peak-detector based receivers typically determine the 'low' and 'high' levels of the received carrier and adaptively set a threshold between them, as shown in Figure 6. However, when a sufficiently strong on-frequency jamming signal is present during the time when the WWVB signal is at its low amplitude state, the receiver may incorrectly establish that the received signal is at its high state, and would consequently not measure the pulse durations correctly, where the information is encoded. The MSF signal represents such a jammer, because it has an accurately set 60 kHz carrier frequency and is time-synchronized with WWVB.

Moreover, its minute-start marker is represented by a high-level that starts at 0.5 s after the beginning of the minute (and second). This is in direct conflict with the WWVB marker, which is high for only the last 0.2 s of the second. Consequently, an envelope detector that is subjected to a sufficiently strong signal level from MSF may detect this first symbol as a '1' instead of a 'marker', potentially resulting in a failure to decode the entire frame correctly. Naturally, other symbols throughout the frame may be impacted in a similar fashion, as the MSF symbols typically contain a transition to high power as early as 0.1 s or 0.2 s after the beginning of the second, thereby interfering mostly with the recovery of '1' and 'marker' symbols in the WWVB receiver.

Lab experimentation was conducted in order to empirically characterize the impact of in-phase interference in the form of the MSF signal. For this purpose, the MSF signal was emulated and added to the digitally synthesized WWVB signal, while having the capability to control their relative levels. The sum of these two signals was transmitted towards several commercially available products, and their ability to receive was recorded as a function of the relative level of interference, while the SNR was kept high. The experiment showed that the existing products failed to receive once the in-phase MSF interference was above -2 dB with respect to the WWVB signal, which is very close to the result anticipated by the analysis. Figure 8 is a screen-capture from the oscilloscope used throughout this experiment, where this added MSF signal can be seen.

ADDRESSING THE RANGE/COVERAGE CHALLENGES

In order to effectively address the coverage problems while operating just a single broadcasting station in Fort Collins, NIST is introducing a new approach that involves adding phase modulation (PM) to the WWVB broadcast while maintaining the existing AM code, so as not to impact the existing time-of-day radio controlled clock devices. However, the addition of PM can adversely affect any device that extracts the carrier from the WWVB signal as a source for a stable frequency by use of a phase locked loop (PLL).

NIST has been conducting surveys to allow users to specify their usage of the WWVB broadcast, and it appears that it is now seldom used as a stable frequency reference, in light of the many low-cost alternatives available for such purpose nowadays. Nevertheless, it is still possible to implement a

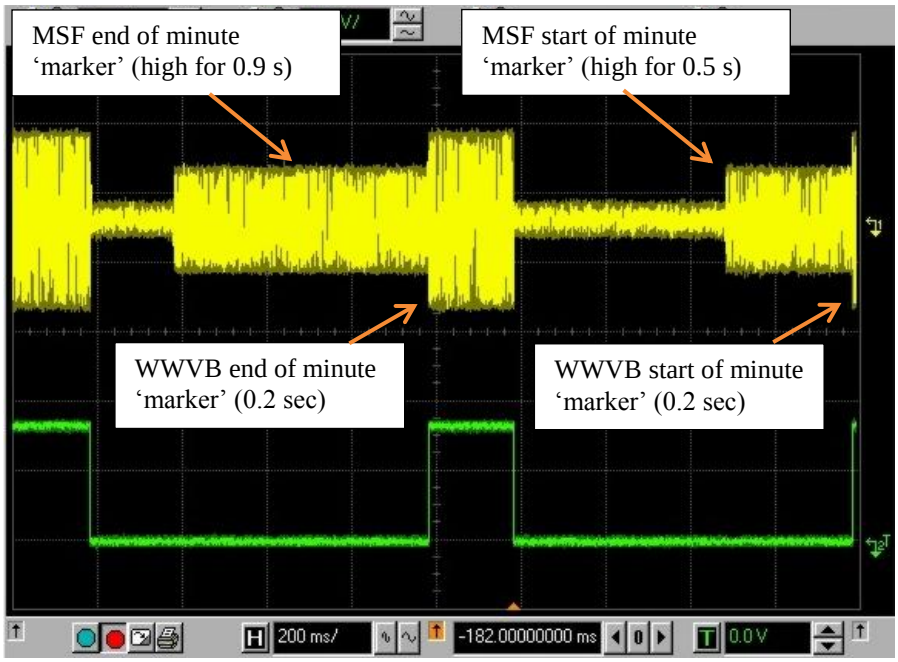

Figure 8. Oscilloscope screen-capture from lab experiment of WWVB operation with MSF interference.

frequency reference based on the carrier extracted from a BPSK signal by employing any of the known schemes for carrier recovery, such as squaring and a Costas loop **[9,10]**.

A NIST Small Business Innovation Research (SBIR) grant was awarded to the Dallas-based company Xtendwave, whose research proposal addressed potential modulation and coding techniques for WWVB and a new receiver technology. Various portions of this research were conducted in collaboration with academia, involving the ElectroScience Laboratory of The Ohio State University and the Southern Methodist University in Dallas, Texas. The following section provides a description of the fundamentals of the new protocol that has been developed for WWVB, compares it against the AM-based protocol, and lists some of the performance benefits arising from its modulation scheme and encoding of the information. The new protocol maintains backward compatibility, as it is imperative that all existing time-of-day radio receive devices continue to operate at the same level of functionality.

It should be noted that the information in the following sections is part of ongoing research, and is presented here only for the sake of comparative analysis.

FUNDAMENTALS OF THE NEW PROTOCOL FOR WWVB

BINARY PHASE SHIFT KEYING MODULATION

The existing WWVB system transmits a pulse-width modulated amplitude-shift keyed waveform on a 60 kHz carrier. The one-second duration '0' and '1' symbols are represented by a power reduction of 17 dB at the start of the second for 0.2 s and 0.5 s, respectively **[8]**. Figure 9 shows the baseband waveforms for the '0' and '1' symbols, where they are denoted $x_0(t)$ and $x_1(t)$ respectively. The additional phase modulation being added to the signal is binary-phase-shift-keying (BPSK), having a 180^o difference in the carrier's phase between the '0' and '1' symbols. Hence, the modulated waveforms representing these symbols may

be expressed as the products of the sinusoidal 60 kHz carrier and the baseband waveforms $s_0(t) = x_0(t)$ and $s_1(t) = -x_1(t)$, respectively, as shown in Figure 9. As can be seen in the figure, the enhanced modulation scheme can be accomplished through simple sign inversion for the waveform representing the '1' symbol. It should be noted that since the existing envelope-detector based receivers do not consider the carrier's phase, they are not impacted by this modification.

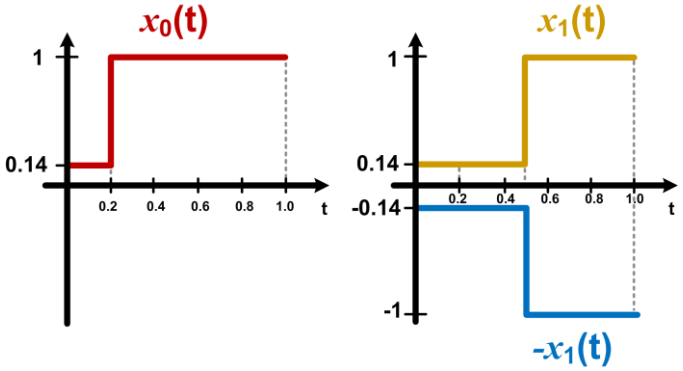

Figure 9. Baseband representation of the '0' and '1' symbols in historical and new WWVB modulations.

A signal-space diagram for the two waveforms of the new PM scheme versus those of the historical one is illustrated in Figure 10. As can be seen in the diagram, the new pair of waveforms, x_0 and $-x_1$, having the same amount of energy (corresponding to their distances from origin), exhibit a much greater distance between the '0' and '1' symbols, allowing for more robust reception in the presence of additive noise. It is to be noted that the existing symbols are strongly correlated, i.e., have a very short distance between them in the signal space with respect to their energies.

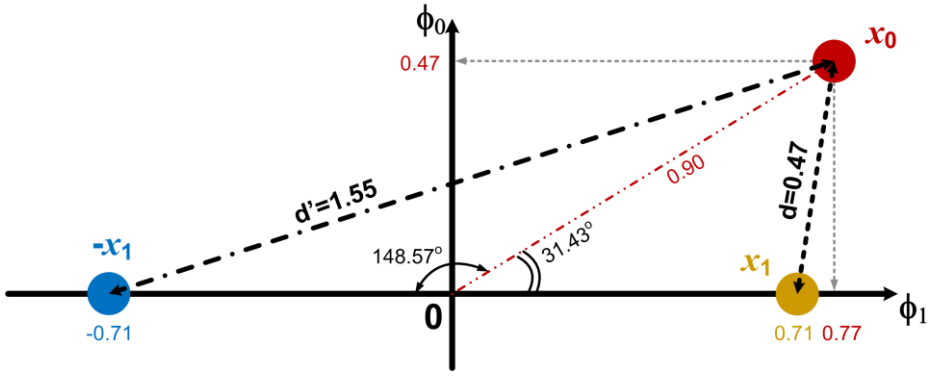

Figure 10. The signal-space representation of the historical and new WWVB '0' and '1' signals.

The Euclidean distance between the two AM waveforms is shown to be 0.47, whereas the Euclidean distance for the two PM waveforms increases to 1.55. Therefore, the *modulation gain*, denoted m_g, representing the power ratio by which the detection capability in the presence of additive noise is improved, is given by

$$m_g = 20 \cdot \log_{10} (1.55 / 0.47) = \mathbf{10.36\ dB}$$

Thus, by simply adding such phase modulation, an order of magnitude of improvement may be achieved when assuming additive white Gaussian noise (AWGN). This analysis implicitly assumes that the receivers for both schemes would be optimal, i.e., based on correlation or matched filtering. In practice, the BPSK receiver may be implemented digitally in a near-optimal fashion, whereas the receivers for the existing

scheme, not designed as a classical digital-communications system, are based on envelope detection, as previously noted. This adds an additional gap of 2 to 4 dB between the two, when only AWGN is considered. However, in the presence of on-frequency interference, the gain offered by realizing a near-optimal BPSK receiver may be arbitrarily higher, as is shown below. Furthermore, additional gains can be offered, as is shown in the following sub-sections, through encoding of the information, use of a known synchronization sequence, and extended-duration reception in the receiver.

It is to be noted that PM, at a rate higher than 600 bit/sec, has been employed by the equivalent broadcast in Germany (DCF77, centered at 77.5 kHz) for several decades **[11]**. The high-rate data that is phase modulated contains a known sequence having good autocorrelation properties, which allows for higher resolution of timing to be extracted from a received symbol, where the entire sequence is embedded. The magnitude of phase modulation applied there, set at ±13°, ensures that the modulated signal is contained within a narrow bandwidth and does not escape the narrow filtering in typical receivers, which is on the order of 10 Hz. This narrowband PM is not comparable in performance to antipodal BPSK, where the two symbols are 180° apart (i.e., exhibiting a correlation factor of -1), but its reception only involves identification of the known sequence through a correlation operation and not the recovery of unknown data.

Figure 11 illustrates, in the form of a simplified block diagram, how a coherent BPSK optimal receiver may be implemented digitally. The filtering of the signal is based on the correlation operation, which is followed by a decision that is made in the presence of AWGN. The bit-error-rate (BER) performance of the receiver, for a signal to noise ratio E_b/N_o, is given by:

$$BER = Q\left(\sqrt{\frac{2 \cdot E_b}{N_o}}\right),$$

where E_b is the energy per bit and N_o is the noise density **[9]**.

The E_b/N_o ratio is equivalent to the ratio between the power of the signal and the power of the noise in a bandwidth that is equal to the bit rate, i.e., $E_b/N_o = SNR \text{ @ } BW=R_b$, where R_b represents the bit rate. The threshold decision block shown in the block diagram is where the decisions are made and the errors occur, in direct relation to the variance of noise, which is shown to have Gaussian nature and equal variances around the '0' and '1' symbols. The BER may also be expressed as a function of the distance between the symbols in the signal space, as follows:

$$BER = Q\left(\sqrt{\frac{d^2}{2 \cdot N_o}}\right),$$

where $Q(x)$ is the tail probability of the normal distribution, i.e.

$$Q(x) = \frac{1}{\sqrt{2\pi}} \int_x^{\infty} \exp\left(-\frac{u^2}{2}\right) du.$$

As previously noted, the analysis presented for the improvement obtained through the introduction of the phase modulation scheme assumed only the presence of AWGN in the receiver. In the presence of RFI, from MSF specifically, the performance improvement could be much more significant and stems from the structure of the BPSK receiver, where the demodulation is based on correlation.

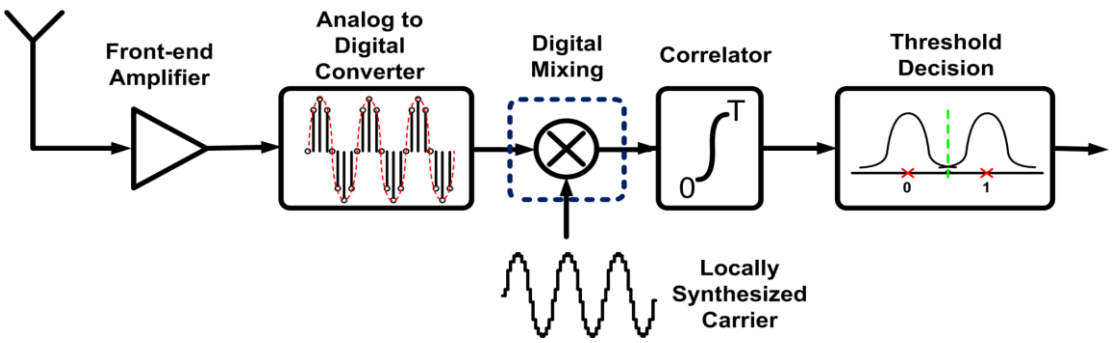

Figure 11. A digital receiver architecture for BPSK.

Figure 12 shows a signal space wherein the constellation for antipodal BPSK comprises the two signals x_0 and x_1 representing the symbols '0' and '1' respectively, having a distance d between them. Although an on-frequency jammer is an aggressor to the system and not an information signal in it, it may be directly represented on this diagram, as it can be expressed as a linear combination of the functions spanning this space (orthogonal sinusoids centered at 60 kHz). This jammer, as shown in the diagram, can be added in vector form to each of the system's two signals x_0 and x_1, resulting in the sums x_0' and x_1' respectively. The distance between these two sums in the signal space, denoted d', is shown to be equal to d, thereby allowing the receiver to operate without any performance degradation. In other words, the on-frequency jammer shifts the signal constellation only by a vector corresponding to its level and relative phase, without reducing the Euclidean distance between the symbols '0' and '1', such that the reception performance is not degraded at all. This holds true, as long as the decision threshold is adjusted according to the jammer, and no nonlinear effects are experienced in the receiver's front-end.

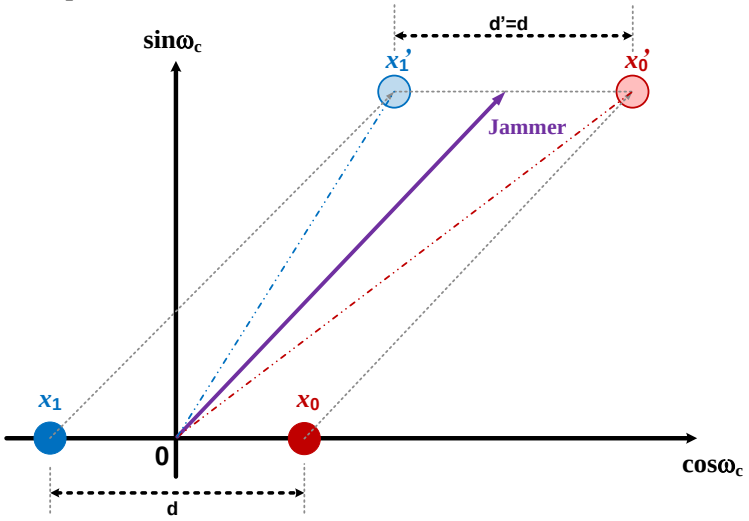

Figure 12. The effect of on-frequency RFI shown in the signal space as a vector diagram.

General Approach to Bit-Designation in the Transmitted Frame

The addition of phase modulation alone offers a significant improvement in performance in the presence of AWGN and RFI, as was shown in the previous subsections. However, the system will benefit further from encoding different information in the phase modulation than that provided through the historical amplitude/pulse-width modulation. In order to maximize such benefits, the most common usages of the received signal have been considered, with the following assumptions being made:

1. The received signal serves to convey the time of day (and date) to those devices that have not yet acquired it, such as a new wall-clock that is powered on for the first time. In this scenario, the greatest amount of completely unknown data is assumed to be conveyed, for which the greatest receiver effort is to be expected. Once time (and all other information) is acquired, the RCC device would have its own time-keeping capability and should not be required to repeat such acquisition. This information, comprising numerical data that represents the date and time of day, will hereafter be referred to as ***time*** *information*.

2. Periodically, devices that have already acquired the time-of-day would rely on the received signal to simply compensate for whatever time-drifts that may have been experienced due to the inherent frequency error in their crystal-based oscillator (typically on the order of ±10 ppm). Naturally, this would be the most common use of the WWVB signal, since a device may require very few acquisition operations in its lifetime, but would regularly depend on the periodic time-adjustments based on the WWVB signal. This information, wherein a specific instance in the transmitted signal represents the timing of interest, e.g., the beginning of a minute, will hereafter be referred to as ***timing*** *information*.

3. Advance notification of the upcoming daylight saving time (DST) transition, i.e., when DST is to end or begin, is advantageous, as it allows the receiving device to perform the one-hour time shift at the correct instance without having to receive the WWVB signal around the time of the transition. In devices that display the time and/or control systems in accordance with it (e.g., pool controllers, irrigation systems), it is obviously important for the correct time to be considered. However, devices that simply need to maintain synchronicity with one another may not need this. Other information that falls under this category is the advance notification of an imminent leap second. The DST schedule and leap second notification information are hereafter referred to as *additional information*. Additional optional messages, for emergency or other purposes, may be lumped into this category as well.

For each of the three types of information listed above, having a different purpose and criticality associated with it, an efficient and robust way for representing the information was devised. This was done under the constraint of the same 60-second frame defined in the historical protocol, while also considering the marker symbols in it. However, the marker symbols, having a duration of only 0.2 s of high power, contain less energy. Hence, their use has been avoided in conveying information and was limited to known components of a synchronization word, as shown in Table 1. While three of the seven markers are within the fixed synchronization word, the four remaining marker symbols are reserved (denoted 'R' in Table 1) and their use is not defined here.

REPRESENTATION OF TIMING INFORMATION USING A KNOWN SEQUENCE

Extracting timing from a digitally modulated received signal is best accomplished when a known sequence, having good autocorrelation properties, is embedded within it. This allows for a correlation operation in the receiver to reveal the timing of the received signal even in low SINR conditions, for which the recovery of individual bits within the sequence might have involved high error probabilities. The successful identification of the known sequence does not require the recovery of the individual bits comprising it, and directly corresponds to the total energy in the known sequence, which is proportional to its duration. Therefore, the duration of the known sequence in the frame is maximized, while weighing this against the need to send the time information in a robust fashion, i.e., with redundancy. As can be seen in Table 1, a total duration of 14 seconds is allocated to the known sequence, starting from the last second of a frame and ending 13 seconds into the next frame. Hence, the amount of energy invested in the timing information is on the order of a quarter of the total energy in a minute frame.

Table 1. Bit-Designation in New vs. Historical WWVB One-Minute Frame.

Second	**0**	**1**	**2**	**3**	**4**	**5**	**6**	**7**	**8**	**9**
Amplitude	Marker	Min[6]	Min[5]	Min[4]	0	Min[3]	Min[2]	Min[1]	Min[0]	Marker
Phase	sync[12]	sync[11]	sync[10]	sync[9]	sync[8]	sync[7]	sync[6]	sync[5]	sync[4]	sync[3]

Second	**10**	**11**	**12**	**13**	**14**	**15**	**16**	**17**	**18**	**19**
Amplitude	0	0	Hour[5]	Hour[4]	0	Hour[3]	Hour[2]	Hour[1]	Hour[0]	Marker
Phase	sync[2]	sync[1]	sync[0]	timepar[4]	timepar[3]	timepar[2]	timepar[1]	timepar[0]	hour[19]	R

Second	**20**	**21**	**22**	**23**	**24**	**25**	**26**	**27**	**28**	**29**
Amplitude	0	0	Day[9]	Day[8]	0	Day[7]	Day[6]	Day[5]	Day[4]	Marker
Phase	hour[18]	hour[17]	hour[16]	hour[15]	hour[14]	hour[13]	hour[12]	hour[11]	hour[10]	R

Second	**30**	**31**	**32**	**33**	**34**	**35**	**36**	**37**	**38**	**39**
Amplitude	Day[3]	Day[2]	Day[1]	Day[0]	0	0	DUTS[2]	DUTS[1]	DUTS[0]	Marker
Phase	hour[9]	hour[8]	hour[7]	hour[6]	hour[5]	hour[4]	hour[3]	hour[2]	hour[1]	R

Second	**40**	**41**	**42**	**43**	**44**	**45**	**46**	**47**	**48**	**49**
Amplitude	DUT[3]	DUT[2]	DUT[1]	DUT[0]	0	Year[7]	Year[6]	Year[5]	Year[4]	Marker
Phase	hour[0]	min[5]	min[4]	min[3]	min[2]	min[1]	min[0]	dston	leap	R

Second	**50**	**51**	**52**	**53**	**54**	**55**	**56**	**57**	**58**	**59**
Amplitude	Year[3]	Year[2]	Year[1]	Year[0]	0	LYI	LSW	DST[1]	DST[0]	Marker
Phase	dlpar[2]	dlpar[1]	dlpar[0]	dst[5]	dst[4]	dst[3]	dst[2]	dst[1]	dst[0]	sync[13]

Since the timing adjustment operation is more frequent and indispensible (assuming that the initial setting of the time may also be accomplished manually or by other means), it is useful to allow it to take place at SINR values that are below the minimum required for reliable acquisition. This justifies a long synchronization word. If the correlation operation in the receiver were to be limited to when the signal is at high amplitude, then the total duration of useful correlation would be at least 7 seconds (the presence of a few 0.2 s AM markers in the synchronization word is compensated by the presence of three AM symbols that are fixed at zero, for which the high-amplitude duration is 0.8 s).

When the timing of the received signal is known to within a defined maximal timing error, the correlation operation may be limited in time accordingly, allowing the design of the known waveform to exhibit good autocorrelation throughout that entire correlation interval. However, when the timing is not known at all (e.g., when acquiring the time or when excessive drift has been experienced since the last successful timing adjustment), the correlation operation is more challenging, as it may be impractical to guarantee that the known sequence would exhibit minimal correlation with all possible values of the unknown data, to minimize the chances of incorrect identification. Figure 13 shows the probability of correct identification of a barker sequence of 11-bits, having good autocorrelation properties, for different SNR values, as measured in a bandwidth of a single bit. As can be seen in the figure, even for 0 dB, i.e., when the signal's power is equal to that of the noise in a 1 Hz bandwidth, the barker sequence would be identified to within 0.25 seconds of accuracy with over 90 % probability (the sum of the three central results in the histogram). The probability of the synchronization resulting in an error of 1 second or more is negligible at such SNR (i.e., below 0.1 %). The consequences of such a rare event can be avoided by considering a measure of confidence that may be generated in the receiver based on reception conditions.

Since the reception of the synchronization word is necessary for the extraction of both the timing and the time information from a frame, future extensions to the protocol become possible, wherein a different synchronization word may be used. This will allow a receiving device to ignore the data fields that follow the synchronization word whenever the data does not represent the time. As long as the amplitude/pulse-width modulation on the signal are unaffected by this, the full backwards compatibility is maintained even during the frames whose phase modulation does not necessarily represent the time.

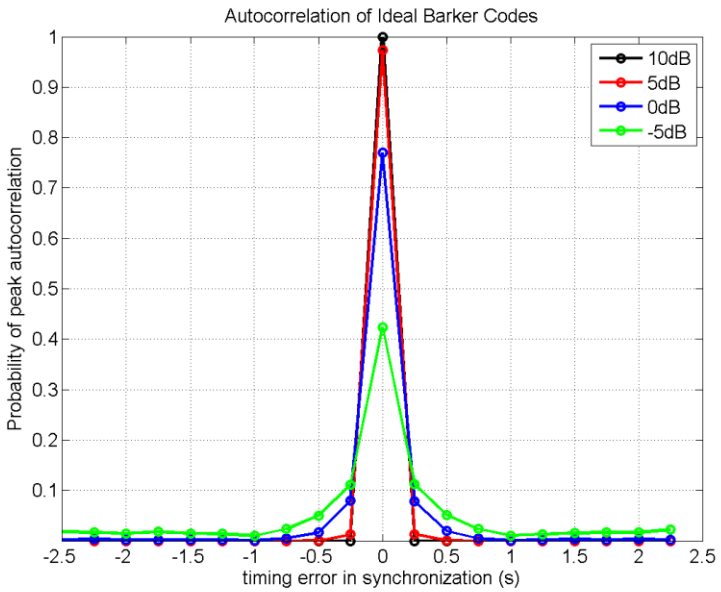

Figure 13. Timing identification probability histogram for an example 11-bit barker code.

EFFICIENT REPRESENTATION OF TIME INFORMATION

Rather than allocating a separate field to each element of time and encoding this information in BCD, as is done in the historical protocol, where a total of 31 bits are consumed, the time may be represented more efficiently and robustly in one merged word, as described below.

The entire time word, which includes the minute, hour, and date, is allocated a total of 26 bits, to which five redundant parity bits are added, totaling a length of 31 bits. Although, coincidently, equal in length to the total used for the representation of time in the historical protocol, it offers great redundancy.

Within the 26-bit time word, six bits are designated to the minute counter (0-59) and the remaining 20 bits represent the number of hours that have elapsed since the beginning of the century.

The number of hours in a century is limited to $100 \times 365.25 \times 24 = 876{,}600$. Therefore, the 20-bit field is used efficiently, since $\log_2(876600) = 19.74$. The 6-bit portion representing the minute is also used efficiently, since $\log_2(60) = 5.9$, which is very close to 6 (60 of the possible 64 combination are used).

It would have been possible, instead, to specify the minute in the century, but this would have required the same number of bits, whereas the separation of minutes allows for some advantages on the receiver side, particularly when considering reception over multiple minute-frames, which is described later.

LINEAR CODING OF TIME WORD

The 26-bit time word is encoded into a 31-bit code-word by use of a Hamming systematic block code **[9]**. This linear block code has the capability to correct a single error that may occur in any of the 31 bits, and the capability to detect up to two errors. If three errors were to occur, the received 31-bit word may appear like a legitimate one, resulting in erroneous decoding. Such scenario is considered intolerable; therefore, the system is designed to minimize its probability. If, for example, the BER is on the order of 10^{-2} (1 %), the probability for three errors is on the order of 10^{-6}.

The block code that was chosen is a *systematic* code, which means that the input data is embedded in the encoded output and may be read directly from there without necessitating decoding. This property does not come at the cost of performance, while it allows for simplified testing and reception (i.e., elimination of the decoding procedure, particularly for high SNR). A block code may be denoted as a (*n*, *k*) code, where *n* and *k* denote the code-word size and the number of information bits respectively. For the time word $n = 31$ and $k = 26$. The equations below specify how each of the 5 parity bits, denoted "time par[*i*]" (*i* = 0, 1, 2, 3, 4), is to be calculated by use of the 26 bits comprising the minute counter (6 bits), and the hour counter (20 bits), which are jointly denoted "time[*k*]" (*k* = 0, 1… 25).

- time par[0] = $\text{sum}_{(\text{modulo } 2)}$\{time[23, 21, 20, 17, 16, 15, 14, 13, 9, 8, 6, 5, 4, 2, 0]\}
- time par[1] = $\text{sum}_{(\text{modulo } 2)}$\{time [24, 22, 21, 18, 17, 16, 15, 14, 10, 9, 7, 6, 5, 3, 1]\}
- time par[2] = $\text{sum}_{(\text{modulo } 2)}$\{time [25, 23, 22, 19, 18, 17, 16, 15, 11, 10, 8, 7, 6, 4, 2]\}
- time par[3] = $\text{sum}_{(\text{modulo } 2)}$\{time [24, 21, 19, 18, 15, 14, 13, 12, 11, 7, 6, 4, 3, 2, 0]\}
- time par[4] = $\text{sum}_{(\text{modulo } 2)}$\{time [25, 22, 20, 19, 16, 15, 14, 13, 12, 8, 7, 5, 4, 3, 1]\}

Syndrome-based decoding, wherein a syndrome vector is calculated based on the received word in a linear fashion, may be used in the receiver. A non-zero syndrome indicates that at least one error occurred in the received word. For this Hamming code, the syndrome can correctly indicate the error location if only one error occurs in the received word. In order to guarantee the reliability of the recovered information, the receiver does not necessarily have to correct the received word when the syndrome is non-zero. Instead, a second reception, confirming the contents of the first, may be used, resulting in increased reliability, at the cost of delayed acquisition. Hence, the error detection capability may be considered more important than the correction capability. Since it is probable to have more than one error in the received word in low SNR scenarios, an erasure may occur and the receiver can make a second acquisition attempt. In contrast, a correction can be made in a high SNR scenario, where the likelihood of having two or more errors is very low, e.g., in the presence of impulsive noise. Whenever at least one bit in a word is recovered in error despite the coding, this represents a word-error event, for which the word-error-rate (WER) is defined. The WER comparison for the coded and uncoded time-word is shown in Figure 14. It should be noted that a WER of 10^{-3} corresponds to one error in 100 years, even if time acquisition is performed 10 times in a year. The demodulation SNR for this WER is shown to be about 8.9 dB for the uncoded word and 6.4 dB for the coded word, representing a coding gain of 2.5 dB.

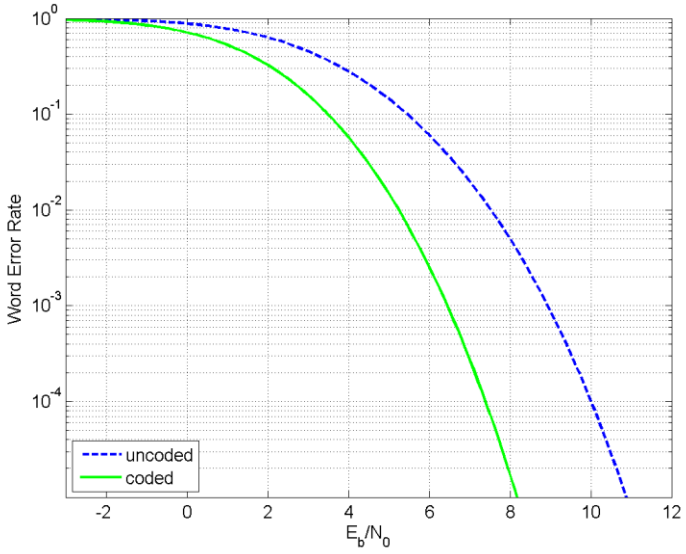

Figure 14. Word error rate comparison for the coded and uncoded time word

ENCODING OF THE ADDITIONAL INFORMATION FIELDS

The 7-bit *additional information* field comprises one bit indicating whether DST is in effect or not, one bit indicating whether a leap-second is to be added at the end of the current half-year, and a 5-bit DST schedule word, which serves to notify of the time and day for the next DST transition. If DST is in effect (e.g., in July), then the interpretation of the 5-bit word should refer to when it is to end. If DST is not in effect (e.g., in December), the interpretation should refer to when it is to start again. The start date and end date options are listed in Table 2 below. A total of 8 specific options are supported for each, and an "out of range" possibility is defined, in case the DST schedule is changed in the future to a time that is not within those covered by the table. Additional options are defined to allow for DST to be implemented permanently or to be cancelled altogether. With three possible values for the time at which the DST transition is to occur (1 AM, 2 AM, or 3 AM) and a 4th option to be used for special messages, as shown in Table 3, a total of 32 combinations may exist for the DST 5-bit schedule word.

Table 2. Designation of bits 0-2 in 5-bit word for DST schedule.

bit 2	bit 1	bit 0	column A	column B (end of DST)	column C (start of DST)
0	0	0	DST permanently off	3rd Sunday before "O"	6th Sunday since "M" (*)
0	0	1	DST permanently on	2nd Sunday before "O"	7th Sunday since "M"
0	1	0	DST out of range	1st Sunday before "O"	8th Sunday since "M"
0	1	1	reserved	last Sunday of Oct. = "O"	1st Sunday of March = "M"
1	0	0	reserved	**1st Sunday of Nov.**	**2nd Sunday since "M"**
1	0	1	reserved	2nd Sunday of Nov.	3rd Sunday since "M"
1	1	0	reserved	3rd Sunday of Nov.	4th Sunday since "M"
1	1	1	reserved	4th Sunday of Nov.	5th Sunday since "M" (*)

(*) The first Sunday in April could be either the 5th or 6th Sunday since the beginning of March.

Table 3. Designation of bits 3 and 4 in 5-bit word for DST schedule.

bit 4	bit 3	significance
0	0	use column A to decode bits 2:0 (special messages)
0	1	next DST transition hour is 1AM, day is in bits 2:0
1	0	next DST transition hour is 2AM, day is in bits 2:0
1	1	next DST transition hour is 3AM, day is in bits 2:0

The Sundays in column C, indicating the start date of DST, are not in chronological order, since it was advantageous to designate the same word to the 1st Sunday of November and to the 2nd Sunday of March, being the current end and start dates respectively. This allows for more efficient representation of the information under the assumption that this DST schedule, which is currently in use, will likely remain the schedule for many years to come. The other optional schedules were defined to allow some margin around what appears to be a possible schedule that would be instated in the future. It is to be noted that the last Sunday in October or in March may be either the 4th or the 5th Sunday of that month.

The 2-bit word comprising the DST status bit and the leap-second notification bit may be used immediately upon reception and is of high importance. These bits are also somewhat unpredictable, and, therefore, have high information content. Hence, this 2-bit word is encoded into 5 bits by use of a shortened Hamming systematic code that provides relatively high robustness, as detailed in the next subsection. In contrast, due to the highly disparate *a priori* probability for the DST transition schedule options, a non-linear code is used to encode the 5-bit DST schedule word into a 6-bit code-word, offering non-uniform distancing for the various code-words, with the most probable one having the highest protection, i.e., the greatest Hamming distance from all other code-words.

LINEAR CODING FOR DST AND LEAP SECOND INDICATORS

The (5,2) shortened Hamming systematic code that is used to encode these two information bits into a 5-bit code-word is derived from a (7,4) Hamming systematic code. The equations below specify how each of the three parity bits, denoted "dlpar[i]" (i = 0, 1, 2), is to be calculated using the two input bits, which are denoted ***dston*** and ***leap***.

- dlpar[0] = dston
- dlpar[1] = sum$_{(\text{modulo } 2)}${leap, dston}
- dlpar[2] = leap

Figure 15 shows the performance gain obtained through the use of this linear code. As can be seen there, at WER=10^{-3}, corresponding to one error in 100 years if time acquisition is performed 10 times in a year, the demodulation SNR is shown to be about 7.3 dB for the uncoded word and 4.3 dB for the coded word, representing a coding gain of 3 dB.

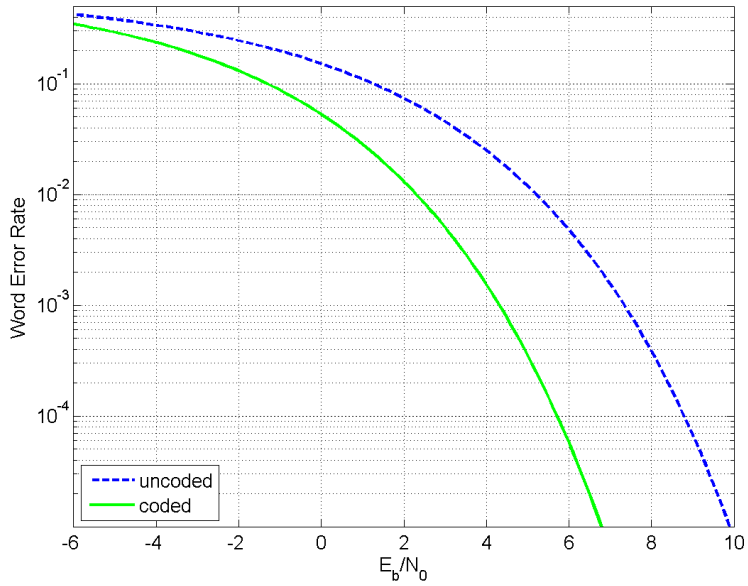

Figure 15. Word error rate comparison for the coded and uncoded DST and leap second indicators.

NONLINEAR CODING OF DST SCHEDULE WORD

The nonlinear code for the advance notification of the next DST transition is designed such that one particular code-word will have maximum protection, corresponding to a maximal minimum Hamming distance, denoted d_{min}. The remaining code-words were selected to have a maximal number of code-words of second maximum d_{min}. Table 4 shows the code-words and their d_{min}. The first code-word, having a maximum d_{min} of 3, is mapped to the most probable DST schedule, which is the one instated most recently (i.e., the DST period starting on the 2nd Sunday of March and ending on the 1st Sunday of November, as shown in green in Table). It is also assumed that the transition will most likely remain at 2 AM, and therefore combinations containing that time are assumed to be more probable.

The schedule shown in red in Table 2 represents the one previously in use, which is assumed to have the second highest probability. Hence, these words have been designated code-words with the second highest minimum distance of two, when coded into the 6-bit code-word.

Table 4. The non-linear code for the advance notification of the DST transition

codeword index	input word of 5 bits					output (coded) word of 6 bits						dmin	message
	bit 4	bit 3	bit 2	bit 1	bit 0	bit 5	bit 4	bit 3	bit 2	bit 1	bit 0		
0	0	0	0	0	0	0	0	0	0	0	0	**3**	**1st Sunday of Nov. or 2nd Sunday since "M" at 2AM**
1	1	0	0	0	0	1	1	0	0	0	1	2	"O" or 6th Sunday since "M" at 2AM
2	0	1	0	0	0	1	0	1	0	0	1	2	2nd Sunday of Nov. or 5th Sunday since "M" at 2AM
3	1	1	0	0	0	0	1	1	0	0	1	2	1st Sunday before "O" or "M" at 2AM
4	0	0	1	0	0	1	0	0	1	0	1	2	3rd Sunday of Nov. or 3rd Sunday since "M" at 2AM
5	1	0	1	0	0	0	1	0	1	0	1	2	2nd Sunday before "O" or 4th Sunday since "M" at 2AM
6	0	1	1	0	0	0	0	1	1	0	1	2	4th Sunday of Nov. or 8th Sunday since "M" at 2AM
7	1	1	1	0	0	1	0	0	0	1	1	2	3rd Sunday before "O" or 7th Sunday since "M" at 2AM
8	0	0	0	1	0	0	1	0	0	1	1	2	DST out of range
9	1	0	0	1	0	0	0	1	0	1	1	2	DST permanently off
10	0	1	0	1	0	0	0	0	1	1	1	2	DST permanently on
11	1	1	0	1	0	1	1	1	0	0	0	1	1st Sunday of Nov. or 2nd Sunday since "M" at 3AM
12	0	0	1	1	0	1	1	0	1	0	0	1	"O" or 6th Sunday since "M" at 3AM
13	1	0	1	1	0	1	0	1	1	0	0	1	2nd Sunday of Nov. or 5th Sunday since "M" at 3AM
14	0	1	1	1	0	0	1	1	1	0	0	1	1st Sunday before "O" or "M" at 3AM
15	1	1	1	1	0	1	1	0	0	1	0	1	3rd Sunday of Nov. or 3rd Sunday since "M" at 3AM
16	0	0	0	0	1	1	0	1	0	1	0	1	2nd Sunday before "O" or 4th Sunday since "M" at 3AM
17	1	0	0	0	1	0	1	1	0	1	0	1	4th Sunday of Nov. or 8th Sunday since "M" at 3AM
18	0	1	0	0	1	1	0	0	1	1	0	1	3rd Sunday before "O" or 7th Sunday since "M" at 3AM
19	1	1	0	0	1	0	1	0	1	1	0	1	1st Sunday of Nov. or 2nd Sunday since "M" at 1AM
20	0	0	1	0	1	0	0	1	1	1	0	1	"O" or 6th Sunday since "M" at 1AM
21	1	0	1	0	1	1	1	1	1	1	0	1	2nd Sunday of Nov. or 5th Sunday since "M" at 1AM
22	0	1	1	0	1	1	1	1	1	0	1	1	1st Sunday before "O" or "M" at 1AM
23	1	1	1	0	1	1	1	1	0	1	1	1	3rd Sunday of Nov. or 3rd Sunday since "M" at 1AM
24	0	0	0	1	1	1	1	0	1	1	1	1	2nd Sunday before "O" or 4th Sunday since "M" at 1AM
25	1	0	0	1	1	1	0	1	1	1	1	1	4th Sunday of Nov. or 8th Sunday since "M" at 1AM
26	0	1	0	1	1	0	1	1	1	1	1	1	3rd Sunday before "O" or 7th Sunday since "M" at 1AM
27	1	1	0	1	1	1	1	1	1	0	0	1	reserved 1
28	0	0	1	1	1	1	1	1	0	1	0	1	reserved 2
29	1	0	1	1	1	1	1	0	1	1	0	1	reserved 3
30	0	1	1	1	1	1	0	1	1	1	0	1	reserved 4
31	1	1	1	1	1	0	1	1	1	1	0	1	reserved 5

Since the DST schedule word is followed by the synchronization sequence, it is desirable to let the most probable DST schedule word, in conjunction with the synchronization sequence, have good autocorrelation properties. Therefore, an offset word C will be added to all code-words in Table 4, in order to improve the synchronization performance while maintaining the minimum Hamming distance of the code-words.

EXTENDED RECEPTION

In order to allow for nearly two additional orders of magnitude of performance improvement, which may be critical in low SINR conditions, the polarity of each of the one-minute frames in an hour is differentially modulated by a corresponding bit in a 60-bit hour-synchronization code. The preserved consistency between the polarities of the synchronization word and the information in each of one-minute frames will allow the receiver to resolve the 180-degree phase ambiguity of BPSK reception.

By correlating against multiple consecutive barker codes, the receiver can accurately adjust its timing and can then use recorded data from an entire hour to perform long-term integration for the hour field (soft addition). This provides a gain of 60 (18 dB), which will allow operation at SINR values well below 0 dB (when evaluated in a 1 Hz bandwidth). While the minute field and the parity field for the time-word vary from one minute to the other in the course of an hour, all other fields remain fixed, and simple addition is possible in order to increase the total amount of energy involved in the information recovery. Since the pattern according to which the minute frame is changing is also known, it too can serve in the extended

reception operation. The receiver may determine its timing with respect to the beginning of an hour based on the identification of a portion of the hour-synchronization-word (at least 6 bits, collected over 7 minutes) with or without recovering information from the minute fields in the received frames.

TRIAL BROADCAST AND INTRODUCTION OF THE NEW SYSTEM

An experiment took place in October 2011, during which the phase modulated signal was first broadcast from the station in Fort Collins. With the performance of BPSK receivers being predictable, the main goals of this experiment were to verify that the existing envelope-detector-based receivers are not impacted by the addition of phase modulation and that the transmitter can tolerate the phase-reversals experienced in the BPSK modulation. The experiment was successful in confirming both of these assumptions, allowing for the new broadcasting system to be pursued while still assuring backwards compatibility.

CONCLUSION

Radio-controlled-clock (RCC) devices that rely on the WWVB broadcast have become widely used in recent years. While the station's transmission power has been increased to allow for improved coverage, reception is being challenged by the growing number of sources of electromagnetic interference, amongst other factors that were analyzed here. In particular, the on-frequency interference from the MSF station in the UK has been identified as a particularly challenging jammer for receivers on the East Coast.

In an attempt to cost-effectively address the reception challenges, NIST is introducing a new protocol for the WWVB broadcast, which will preserve its amplitude modulation properties, in order to maintain backwards compatibility and not impact existing devices, while adding phase-modulation that would allow for the greatly improved performance. The information modulated onto the phase contains a known synchronization sequence, error-correcting coding for the time information and notifications of daylight-saving-time (DST) transitions that are provided months in advance.

Furthermore, the new system is scalable in that it allows for receivers experiencing different reception conditions to use the received signal differently. In particular, it is designed to allow for the accumulation of received energy over multiple one-minute frames, to provide for a corresponding gain in the receiver (i.e., reception for a whole hour may provide a gain of 60, or 18 dB, with respect to a single minute).

All of these improvements serve to greatly increase the robustness and reliability of this communication system, allowing it to operate at signal-to-noise ratios that are over two orders of magnitude lower than those required in the existing scheme, while exhibiting even higher gains in scenarios of on-frequency jamming, to which the existing receivers are particularly vulnerable.

A receiver for the new phase-modulation based system may be realized extensively digitally in a complementary metal-oxide-semiconductor (CMOS) integrated circuit. This allows for the elimination of external passive components that are currently found in RCC devices and also for the integration of such receiver within a larger system-on-chip (SoC), where it may represent a small portion of the overall silicon die. Such realization of the receiver, and the much improved performance that it will exhibit, will allow for greatly wider usage of the WWVB broadcast in many applications where time-keeping, and/or synchronization are needed.

ACKNOWLEDGEMENT

The work presented here was partially supported by the National Institute of Standards and Technology under SBIR Grants # SB1341-10-SE-0700 and NB401000-11-04154, as well as by the National Science Foundation under Grant # EEC-0946373 to the American Society for Engineering Education.

REFERENCES

[1] M. Deutch, W. Hanson, G. Nelson, C. Snider, D. Sutton, and W. Yates, 1999, *"WWVB Improvements: New Power from an Old Timer,"* in Proceedings of the 31st Annual Precise Time and Time Interval (PTTI) Applications and Planning Meeting, 7-9 December 1999, Dana Point, California, USA (U.S. Naval Observatory, Washington, D.C.), pp. 523-536.

[2] M. A. Lombardi, A. N. Novick, J. P. Lowe, M. Deutch, G. Nelson, D. Sutton, W. Yates, and D. W. Hanson, 2009, *"WWVB Radio Controlled Clocks: Recommended Practices for Manufacturers and Consumers,"* NIST Special Publication 960-14.

[3] J.P. Lowe, 2011, *"We Help Move Time through the Air,"* **Radio World**, March 23, 2011, Vol. 35, No. 8 pp. 69-70.

[4] A.D. Watt, 1967, **VLF Radio Engineering,** (Chapter 3), Pergamon Press.

[5] CCIR (International Radio Consultative Committee), 1986, *"Characteristics and Applications of Atmospheric Radio Noise,"* CCIR Report 322-3, International Telecommunication Union, Geneva, Switzerland.

[6] M. A. Lombardi, 2002, *"NIST Time and Frequency Services,"* NIST Special Publication 432.

[7] Time at NPL *http://www.npl.co.uk/publications/science-posters/time-at-npl*.

[8] J. P. Lowe and K. Allen, 2006, *"Increasing the Modulation Depth of the WWVB Time Code to Improve the Performance of Radio Controlled Clocks,"* in Proceedings of IEEE International Frequency Control Symposium and Exposition, June 2006, Miami, Florida, pp. 615-621.

[9] J. G. Proakis, 2007, **Digital Communications**, McGraw-Hill.

[10] D. P. Taylor, 2002, *"Introduction to 'Synchronous Communications,"* **Proceedings of the IEEE**, **Vol. 90**, No. 8, Aug 2002, 1459-1460.

[11] P. Hetzel, 1988, "*Time dissemination via the LF transmitter DCF77 using a pseudo-random phase-shift keying of the carrier*," 2nd European Frequency and Time Forum.